INVESTIGATION OF FRACTURE PARAMETERS OF CONCRETE INCORPORATING BASALT FIBERS

AHMET ONUR PEHLİVAN *
Department of Civil Engineering, Maltepe University, 34857, Istanbul, Turkey

Concrete is a brittle material that should be enhanced with better tensile strength and toughness capacity. Concrete matrix is generally reinforced with fibers which are extremely helpful inhibiting the crack propagation and supplying the ability of strain accumulation into concrete matrix. In this study, an environment friendly type of fiber was introduced into concrete for the investigation of mechanical properties and fracture characteristics by size independent double-K fracture parameters asserted in the literature. Effect of basalt fibers with different lengths and contents were investigated under notched three-point bending tests and relevant parameters obtained and calculated, were compared for two distinct parameters: fiber length (6, 12, 24 mm) and content (0, 0.1%,0.3%, 0.5%, 1%). Shorter fibers confronted dispersion problems when used in higher content whereas 12 mm fiber specimens performed more stable results. Fracture energy dissipation was found to be linearly increasing with increasing fiber content and also longer fibers were found to be more efficient. Double-K fracture parameters were found to be resourceful when considering toughness and ductility of the material besides these parameters indicated useful information regarding the pre-cracking and post-cracking behavior of concrete. SEM investigations were also conducted to monitor the bonding between basalt fibers and concrete matrix.

Keywords: *Fracture parameters, Basalt fiber, CMOD, Fracture energy, Fiber length*

1. Introduction

Concrete is a good composite material that can detain high amounts of compressive loads whereas tensile strength and strain capacity is relatively very low. Fibers are introduced into concrete as reinforcement filaments that alter the mechanism for tensile stresses exceeding the concrete tensile strength which is known to be minimal. Due to their filament geometry, fibers provide plasticity to enhance the strain attaining capacity of the brittle concrete matrix [1].

Main aim of incorporating fibers into concrete is to provide control of cracking and with the help of bridging action increasing the fracture toughness of brittle cementitious matrix. Bridging action is mainly governed with the debonding, sliding and pulling-out behaviour which are mainly associated with the adhesion between the fiber and the matrix [2].

Fiber diameter is of extreme importance since lower diameter fibers provide more homogenous distribution in the matrix [1]. If resolving the overall homogeneity problem that may show up after fiber addition is set aside, presence of fibers display high potential in reducing the amount of microcracks originated in concrete and decrease the permeability. Besides diameter, fiber length may be an important parameter however, in literature there has been controversial findings regarding fiber length that should be enlightened.

Basalt fiber is a new type of green and healthy green inorganic fiber material that has originated from the igneous rock named basalt. In comparison to other fibers, basalt fibers have several advantages regarding environmental prominence, mechanical performance and chemical stability [3]. However, this superior performance may be tricky when used in a challenging matrix like concrete. Research conducted on basalt fibers used in concrete are limited and erratic. Within some studies, superior characteristical advantages were diagnosed by several researchers primarily on toughness and accordingly on other mechanical properties whereas reduction in several properties were also asserted. The primary target of this study is to reveal the possible enhancement of concrete when basalt fibers were incorporated and thereby highlighting the effect of the fiber length and content on mechanical performance and particularly on the specific fracture toughness parameters asserted by Xu and Reinhardt [4]. Analysis of these size independent fracture parameters is a key concern in structural design ensuring better microcrack control hence increasing the overall life time of structures.

2. Theoretical background

Concrete is a quasi-brittle material which experiences a large stable crack extension before unstable fracturing which is originally called fracture process zone. And fracture behavior of concrete is significantly influenced by the fracture process zone. Many researchers have proposed several models to simulate the softening behaviour and the fracture characteristics in concrete applications. According to Xu and Reinhardt [4], fracture process zone consists of three distinct stages: (i) crack initiation, (ii) stable crack propagation, (iii) unstable fracture as was also manifested in several other studies. To solve the analytical solution of the fictitious crack for quasi brittle materials, a double K is proposed by Xu and Reinhardt. [5]. In double–K criterion,

* Autor corespondent/*Corresponding author*,
E-mail: onurpehlivan@maltepe.edu.tr

two fracture parameters were introduced for different stages of the fracture mechanism and both of them are given in terms of stress intensity factor. K_{IC}^{Q} is called the initiation toughness whereas K_{IC}^{S} is the unstable fracture toughness or the critical stress intensity factor. Initiation toughness (K_{IC}^{Q}) is calculated by determining the initial cracking load (P_{ini}) from the loading sequence and initial crack length which was a test parameter decided prior to testing. Unstable fracture toughness K_{IC}^{S} is calculated by obtaining the maximum load P_{max}, and critical effective crack length. Crack initiation and propagation phases may be followed by checking the toughness of the material. When the toughness value due to loading was lower than initiation toughness, there is no crack development whereas when toughness value is between values of initiation and unstable fracture toughness, stable crack development occurs and when the toughness value due to loading is higher than the unstable fracture toughness, unstable crack development is observed.

2.1. Calculation of fracture energy and double-K fracture parameters

Fracture energy (G_f) is the amount of energy absorbed per unit area of crack in the crack opening direction. Standard method used for calculating the fracture energy is proposed by Hillerborg et al. [6] and can be calculated as the ratio of the total area under the load-CMOD curve of the notched beam to the total crack ligament area as given in RILEM FMC 50 [7] with the following equation:

$$G_f = \frac{W_0}{A} = \frac{W_0}{b(h-a_0)} \quad (1)$$

where is W_0 is the area under the load deflection curve which may be also denoted as the work done by the external load applied on the notched beam, A is the ligament area.

Double-k fracture parameters (K_{IC}^{Q} and K_{IC}^{S}) are evaluated as follows:

$$K_{IC}^{Q} = \frac{3(P_Q + mg\times10^{-2})\times10^{-3} S\sqrt{a_0}}{2bd^2} g(\alpha_0) \quad (2)$$

$$g(\alpha_0) = \frac{1.99-\alpha_0(1-\alpha_0)(2.15-3.93\alpha_0+2.7\alpha_0^{2})}{(1+2\alpha_0)(1-\alpha_0)^{3/2}}, \alpha_0 = \frac{a_0}{h} \quad (3)$$

where K_{IC}^{Q} is the initial fracture toughness (MPa.m$^{1/2}$); P_Q is the first-crack load (N), S is the span length (m), a_0 is the depth of the notch (m), b and d are the width (m) and height (m) of the specimen. First crack load (P_Q) is determined according to ASTM C1018.

$$K_{IC}^{S} = \frac{3(P_{max} + mg\times10^{-2})\times10^{-3} S\sqrt{a_c}}{2bd^2} g(\alpha_c) \quad (4)$$

$$g(\alpha_c) = \frac{1.99-\alpha_c(1-\alpha_c)(2.15-3.93\alpha_c+2.7\alpha_c^{2})}{(1+2\alpha_c)(1-\alpha_c)^{3/2}}, \alpha_c = \frac{a_c}{h} \quad (5)$$

where K_{IC}^{S} is the unstable fracture toughness (MPa.m$^{1/2}$), P_{max} is the initial cracking load (N), S is the span length (m), a_c is the effective critical length (m), b, d and m are the width (m), height (m) and mass (kg) of the specimen.

$$a_c = \frac{2}{\pi}(d+h_0)\arctan\sqrt{\frac{bEV_c}{32.6P_{max}} - 0.1135} - h_0 \quad (6)$$

where h_0 is the thickness (m) of the blade that the extensometer was clipped on; V_c is the critical value of CMOD (μm) that corresponds to maximum load P_{max}, E is the elasticity modulus (GPa).

$$E = \frac{1}{bc_i}\left[3.70 + 32.6\tan^2\left(\frac{\pi}{2}\frac{a_0+h_0}{d+h_0}\right)\right] \quad (7)$$

where c_i (μm/kN) is the initial compliance calculated from the load–CMOD curve.

3. Materials and methods

3.1 Materials

In this study, basalt fibers (BF) were used in producing basalt fiber reinforced concrete (BFRC) specimens. CEM I 42.5 R cement from Akcansa cement factory was used as binder. Basalt fibers were used with different ratios (0, 0.1, 0.3, 0.5, 1.0 by vol.) and length (6, 12, 24 mm) were used in this study. Coarse aggregates used in this study were crushed stone aggregates with a maximum aggregate size of 16 mm whereas natural crushed sand and river sand were used as fine aggregates and also densities were found as 2.68, 2.72 and 2.74 respectively. Properties of basalt fibers are given in Table 1. Properties of cement and fly ash are given in Table 2. Concrete mixture proportions are given in Table 3.

3.2. Testing methods

Mechanical tests were carried out on different steel molds including cylinders and prismatic specimens. Compressive, tensile splitting, flexural strength tests and for fracture testing notched flexural three-point beam tests were adopted. Effect of basalt fiber inclusion with different percentages along with the fiber length on the mechanical properties including fracture characteristics were investigated. Compressive and splitting tensile strength tests were carried out on 100 x 200 cylinder specimens.

Table 1

Properties of basalt fibers.

Diameter (μm)	Length (mm)	Tensile Strength (MPa)	Elasticity (GPa)	Density (kg/m^3)
9-23	6-12-24	4840	89	2700

Table 2

Properties and compositions of cement and fly ash.

Composition (%)	SiO_2	Al_2O_3	Fe_2O_3	CaO	MgO	SO_3	Na_2O	K_2O	LOI	Density (kg/m^3)
Cement	19.81	5.58	3.42	63.70	1.22	3.34	0.24	0.66	1.85	3110
Fly Ash	52.56	26.46	6.77	2.24	2.06	0.20	0.38	4.22	3.30	2380

Table 3

Mixture proportions and slump results

Mixtures	Cement	Fly Ash	Water	Coarse Aggregate (4-8 mm)	Coarse Aggregate (8-16 mm)	Crushed Sand	River Sand	Fiber	SP	Slump
	(kg/m^3)	(kg/m^3)	(kg/m^3)	(kg/m^3)	(kg/m^3)	(kg/m^3)	(kg/m^3)	(kg/m^3)	(kg/m^3)	(mm)
Control	340	57	170	472	430	496	483	0	3.97	150
BF6-1	340	57	170	471	429	495	482	2.7	4.37	125
BF12-1	340	57	170	471	429	495	482	2.7	4.37	130
BF24-1	340	57	170	471	429	495	482	2.7	4.37	130
BF6-3	340	57	170	470	428	493	480	8.1	4.96	125
BF12-3	340	57	170	470	428	493	480	8.1	4.96	135
BF24-3	340	57	170	470	428	493	480	8.1	4.96	140
BF6-5	340	57	170	468	425	492	479	13.5	5.56	125
BF12-5	340	57	170	468	425	492	479	13.5	5.56	140
BF24-5	340	57	170	468	425	492	479	13.5	5.56	150
BF6-10	340	57	170	459	422	490	475	27	7.54	125
BF12-10	340	57	170	459	422	490	475	27	7.54	140
BF24-10	340	57	170	459	422	490	475	27	7.54	155

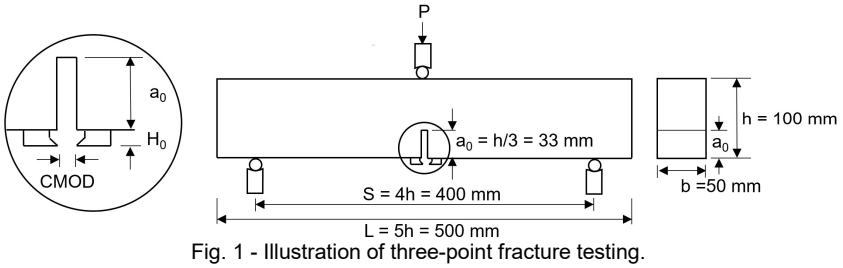

Fig. 1 - Illustration of three-point fracture testing.

Flexural strength tests were conducted on specimens with 100 x 100 x 500 mm beams, whereas flexural toughness was measured with 50 mm x 100 mm x 500 mm specimens. Flexural toughness calculations were held with beams with a notch width of 3 mm in the midspan starting from bottom face of the specimen (Figure 1). Height of the specimen was 100 mm supplying a ratio of S/h = 4 and notch depth was chosen to be 33 mm supplying the ratio of h/a_0 =3. Specimens were loaded under three-point bending test with a clear span of 400 mm with a displacement controlled closed loop servo hydraulic MTS test system with a maximum loading capacity of 100kN at a rate of 0.01 mm/min. Crack mouth opening displacements were measured through the clip-on displacement gage which is easily mounted with the help of the steel knife edges glued to the midcenter of the bottom face of the test specimen. Two linear variable transducers were placed on each side of the specimens to record the vertical deflection of the specimens simultaneously. Test was aborted reaching the crack mouth opening displacement value limit value of 0.2 mm for all specimens.

Microstructural investigations were also conducted for all specimen series. Fragmented pieces that were obtained from mechanical tests were saved for further microstructural analysis. SEM observations were utilized for fiber matrix interactions on Philips XL30 scanning electron

microscope on secondary electron imaging with an accelerating voltage of 15kV.

4. Results and discussion

4.1. Workability

Slump values of all mixtures are given in Table 1. Superplasticizer contents were adjusted to supply adequate slump and same amounts were used for all specimens with similar fiber content. When specimens with similar fiber content were compared it is seen that short fibers cause lower workability. Moreover, this behavior was seen to be more pronounced for specimens with higher fiber content. This may be related to higher number of individual fibers which complicate the uniform distribution of fibers and eventually obstructing the overall workability of the mixture. These findings were found to be consistent with other studies in literature [8] whereas controversial results were seen in another study. Kabay [9] indicated that doubling the fiber length reduced workability and increased the need for superplasticizers for proper placement.

4.2. Compressive strength

Compressive strength results are illustrated in Figure 2. For 0.1% inclusion generally there were no significant change of fiber presence. However, with the increasing fiber content compressive strength results differ from the reference specimens which confirm the effect of fiber addition in compressive strength. As shown in Figure 2, highest compressive strength was achieved for specimens with 0.5 % medium length fibers and the increase was recorded as 3.79%. 6 mm fibers exhibited lower compressive strength than longer fibers which may be related to stronger bridging effect and resistance to pulling out [8]. Highest decrease in the overall results were monitored to be 6.18% which was observed for longer fiber specimens with higher content. Results proved that compressive strength was more prone to fiber content with respect to length. This effect of higher amount of fibers on compressive strength may also be linked with slump results and also it has to be noted that increasing fiber volume also changed the variation in the results and increased the standard deviation in specimens with 1% fiber usage. Higher amount of fibers may have affected the overall integration in the internal structure and may have led to extra voids thus lowering the compressive strength. Furthermore, greater interface zone between the fiber and concrete aggregate influences the restrained concrete zones under uniaxial compression [1]. Similar decreases in compressive strength were also found in similar studies [9, 10].

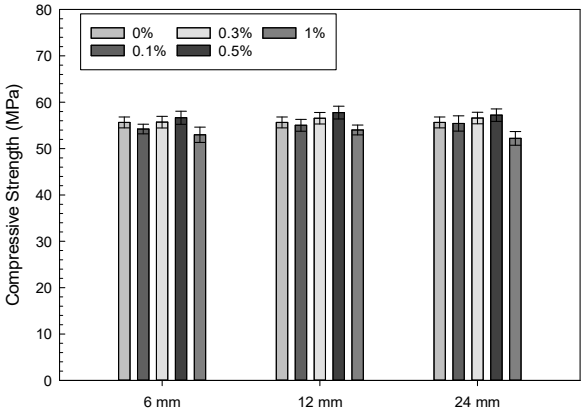

Fig. 2 - Compressive strength test results.

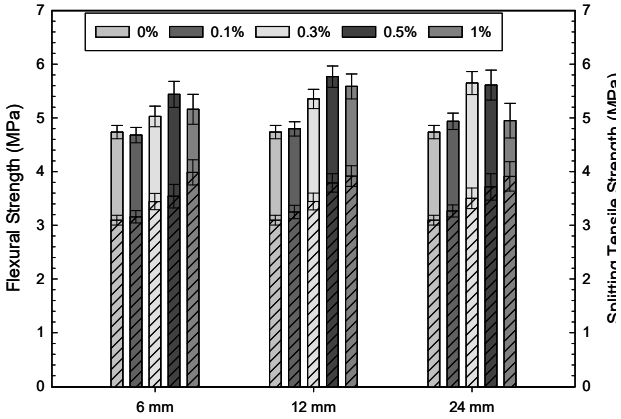

Fig. 3 - Flexural and splitting tensile (textured in the graph) results.

4.3. Splitting tensile strength

Splitting strength results are given in Figure 3 with textured format. For all levels of inclusion, increment in splitting tensile strength was detected. The decisive parameter providing the resistance to splitting tensile forces was ascertained to be fiber content. Increasing fiber content increased the ultimate capacity for all fiber lengths up to a level of 29% that should be interpreted as the bridging action regulating the propagation of microcracks [2]. In contrast to compressive strength results, fiber length was found to be significant when used with high fiber content. Shorter fiber specimens proved to be effective when dealing with direct tensile forces. However, medium length and long fiber specimens also demonstrated close results to shorter fiber specimens. Shorter fibers with higher fiber content exhibited better performance resisting the direct tensile forces acting on a linear segment under splitting with higher number of individual fibers controlling the microcracks and restraining the formation of macrocracks.

4.4. Flexural strength testing

Specimens with the 0.5% fiber content with medium fiber length was found to be effective when flexural strength results were diagnosed and maximum increment in the results was 22%. Also it should be noted for all fiber lengths specimens with 0.5% fiber ratio displayed better performance. Long fiber specimens with high amount of fibers were found to be significantly affected and this may be linked to possible flocculation at the tension zone. Relatively similar condition was observed for shorter fibers (6 mm) which may also be inferred as a flocculation problem considering the number of individual fiber particles when the fibers are short and volume percentage is high. However, in another study, 22 mm fibers were found to be more efficient compared to 12 mm fibers [8]. With the overall findings of the tensile tests, longer fibers exhibited superior bridging effect and stronger pullout resistance however for splitting mechanism distribution of shorter fibers were more efficient [8].

4.5. Load-CMOD curve analysis

As can be observed from Figs. 5, 6, 7, 8 and 9, inclusion of fibers significantly affected the overall fracture performance increasing the peak load and improving the post peak behavior thus signaling tougher structure. Reinforcing concrete with fibers increased the overall fracture energy by 37% for specimens with long fibers and higher fiber content (Figure 4) Results show that increment of the fiber length was more prominent when compared to other mechanical properties. Besides, BF24-10 and BF12-10 specimens attributed higher toughness increase with respect to BF6-10, increase for BF6-10 specimens was limited with 20% hereby it should clearly be inferred that increment in toughness was constricted with fiber length. Also lower amount of longer fibers (both BF24-5 and BF12-5) was found to have higher fracture toughness with respect to BF6-10 specimens. This may be concluded that high volume percentage of shorter fibers were less effective with respect to longer fibers.

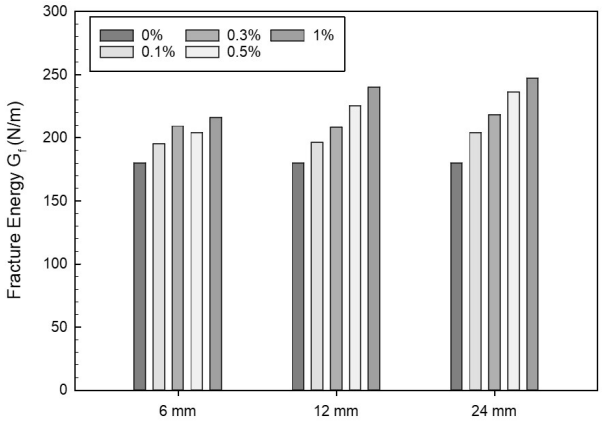

Fig. 4 - Fracture energy results.

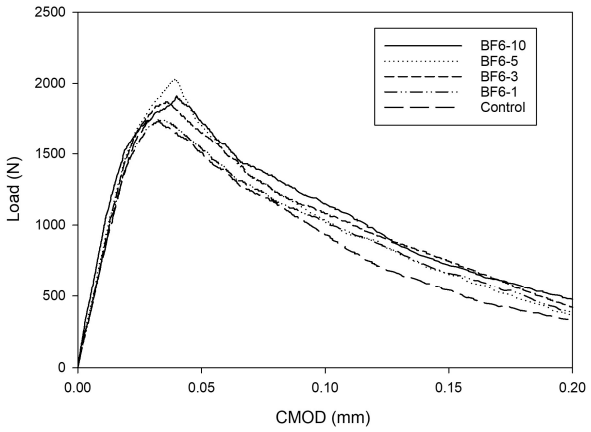

Fig. 5 - Load-CMOD curves for specimens with 24 mm fibers.

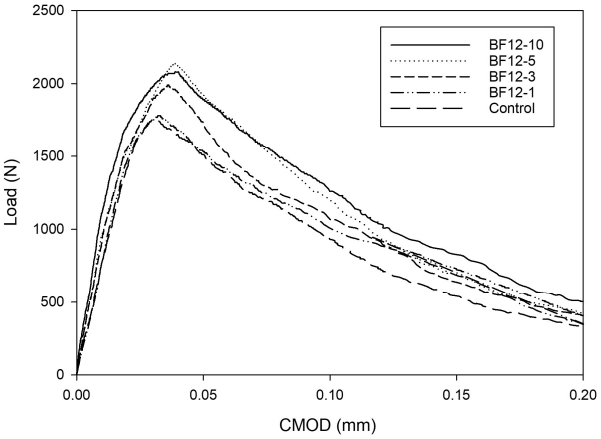

Fig. 6 - Load-CMOD curves for specimens with 12 mm fibers.

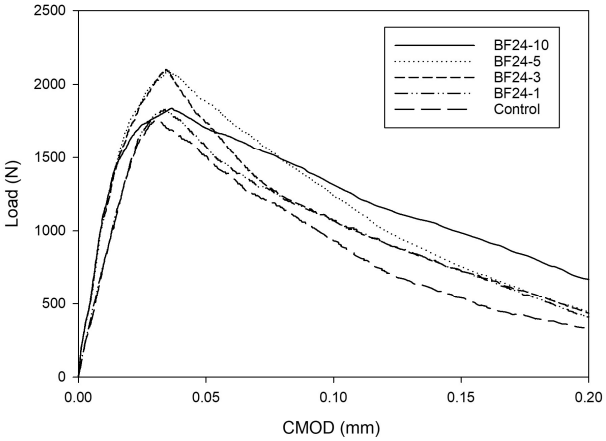

Fig. 7 - Load-CMOD curves for specimens with 6 mm fibers.

Long fibers exhibited superior performance with respect to medium fibers although this behavior was not valid when ultimate flexural tensile tests were considered. This situation was also observed when long and medium fibers were compared with 0.5% fiber content. Also for 3% fiber inclusion, longer fibers have contributed more (21%) than medium length fiber specimens (15%). Also with limited fiber inclusion (0.1%) increment in the toughness was also in favor of the longer fibers. Minimum increase in the toughness was 8% for all fibrous specimens.

BF6-10 specimens exhibited the highest critical CMOD which reflect the crack opening when specimen reached its peak load. This behavior monitors the pre-cracking behavior of specimens with fibers however overall toughness is a measure of both pre-cracking and post-cracking behavior. Superior performance of BF6-10 specimens in CMOD results may be correlated to higher vertical deflection under three point bending and correspondingly higher amount of opening in the bottom of the beam may be based on the shorter fiber length that may have slipped easier than longer fibers so the ability of crack bridging was inadequate [3].

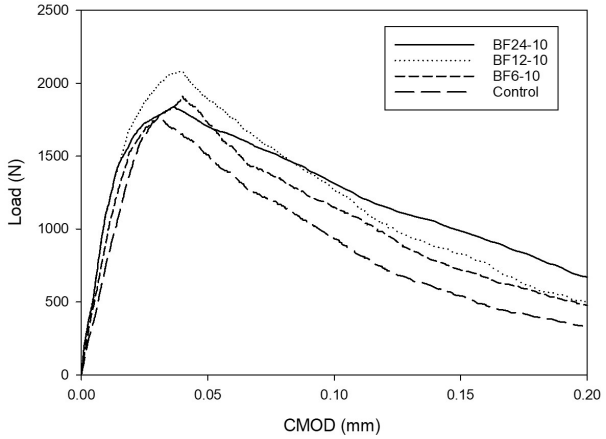

Fig. 8 - Load-CMOD curves for specimens with 1% fiber content.

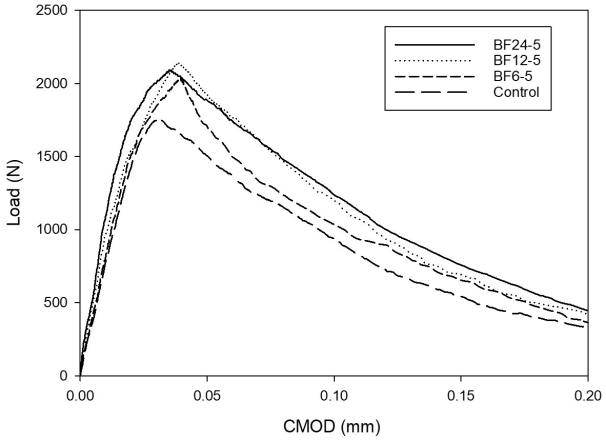

Fig. 9 - Load-CMOD curves for specimens with 0.5% fiber content.

Modulus of elasticity results are calculated by Eq. 7 from initial compliance values obtained from the slope of the load-CMOD curve and given in Figure 10. Long fiber specimens displayed higher modulus of elasticity for 0.3, 0.5 and 1 % which indicates that fiber length is of high significance in this aspect. For all fiber series 1% fiber content showed higher stiffness which can be linked to stronger bridging action of fibers despite high fiber content. This may be viewed as a positive indication for basalt fibers regarding the proper combination with the cementitious composites.

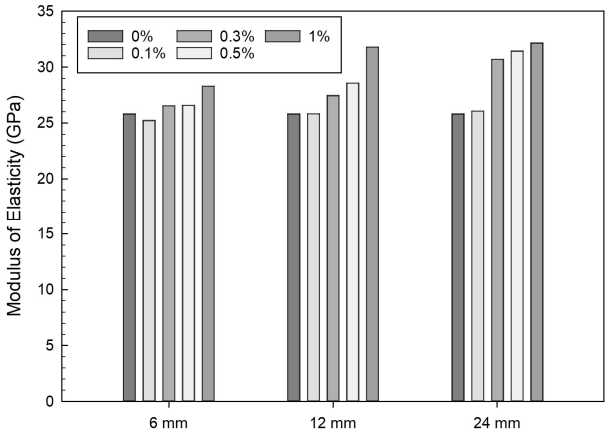

Fig. 10 - Modulus of elasticity results of notched three-point flexural loading tests.

4.6. Double-K parameters

Double K-parameters calculations are used for obtaining the two distinct fracture toughness values that define and characterize the capacity of a material to resist against cracking under flexure loads. These two size-independent fracture parameters provide information about crack initiation and propagation. Initiation toughness (K_{IC}^{S}) indicate the level of toughness of the first cracking and over this level cracks grow stably whereas over unstable fracture toughness (K_{IC}^{Q}), crack growth loses stability which leads to overall failure at the end [4].

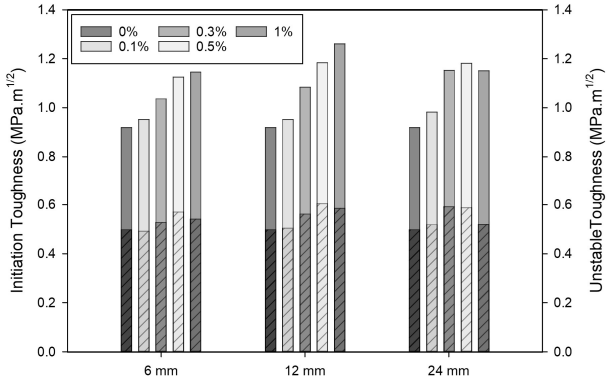

Fig. 11 - Double-K fracture parameters.

Double-K parameters were calculated from the experimental parameters and the mechanical findings of the study and given in Figure 11. When initiation toughness values are inspected, it is seen that specimens with 0.5% fiber content exhibited extreme performance with respect to other fiber content ratios. This may be interpreted as 0.5% is the optimum fiber content for fiber usage. Specimens with longer fibers especially with high amount of fiber usage confronted problems in crack initiation mechanism which have led to earlier cracking in these specimens. It was ascertained that medium length fiber specimens proved out to be the optimum fiber size. According to unstable toughness results, a linear increase was detected

for both short and medium length fibers however behavior of longer fiber specimens was inconsistent. BF12-10 demonstrated the best performance for unstable fracture toughness and 37% increase was monitored for these specimens. Also BF12-5 and BF24-5 specimens displayed 29% increase. These specimens were to resist further cracking that dangers the overall integration of the concrete structure. Both initiation and unstable toughness values were found to be coherent with the experimental studies in the literature. Akturk et al. [11] calculated 0.8 MPa.m$^{1/2}$ ordinary plain concrete whereas for polypropylene fibers were 1.0 MPa.m$^{1/2}$ whereas similar results were found in this study. Sun et al. [12] also investigated similar size independent fracture parameters and found similar values with ranging fiber contents and also in the same study double-K parameters were confirmed to be independent from size effects.

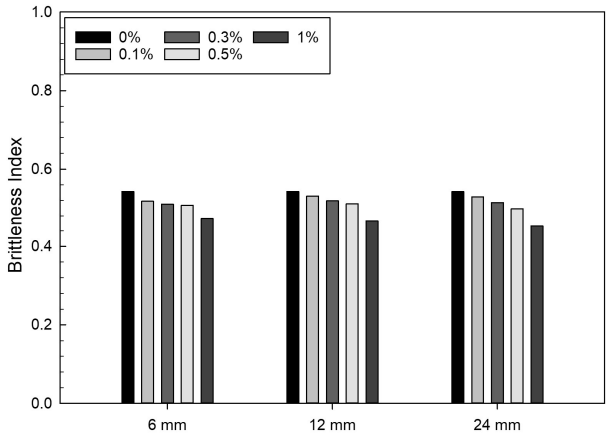

Fig. 12 - Brittleness index values for all specimens.

The comparison of initiation to unstable fracture toughness was monitored for the brittleness index as was proposed by Kumar and Barai [13]. A lower brittle index value signifies higher ductility of the material. According to this classification, BF24-10 specimens exhibited the lowest ratio thus highest ductility between all series as depicted in Figure 12. When diagnosing the overall results, lowest brittle index value specimens were BF24-10, BF12-10 and BF6-10 respectively which gives an important clue about the importance of the fiber content in ductility of the material. Also in this aspect, although not to high extent, long fiber specimens performed better than other fiber sizes. Brittleness index value was 0.54 for plain concrete specimens which was also in agreement with previous studies in literature. Akturk et al. [11] also confirmed the effectiveness of the brittle index calculation.

Critical crack length is also an important parameter defining the crack length triggering the unstable crack growth. From the results given in Figure 13, it is observed that critical crack length was highest for the specimens with the highest fiber content and this was valid for all fiber lengths. It was also noticed that critical crack length was increased with the increase in the fiber length and this effect was more pronounced with higher fiber content specimens. Highest increase in the critical crack length was 15% for BF24-10 specimens.

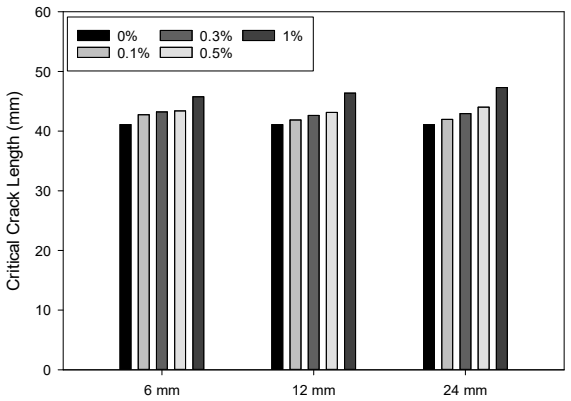

Fig. 13 - Critical crack length values with different fiber content and length.

4.7. Microstructural Investigation

Specimens from all mixtures were investigated under secondary electron scanning electron microscopy and some micrographs are given in Figures 14 and 15. Specimens with higher fiber content were found to have high amount of loose fiber both crushed and have slipped (Figure 14a). And also in several fragments of the specimen fiber dispersion problems were detected especially for short fiber specimens. High amount of hydration products were noticed covering the basalt fiber surfaces which may be deduced as enhanced mechanical bonding and also resistance to slippage by adhesion with the concrete matrix. Also presence of hydration products on fibers were also confirmed by EDX analyses. As the cement matrix starts to fail, basalt fibers started to consume higher stresses and delayed the crack propagation by bridging effect thus increasing the ultimate strength, strain capacity and ductility of concrete [12].

Specimens with higher fiber content also were found to have good matrix structure and no extra voids were detected regarding the presence of excess fibers except BF6-10 specimens. Microstructural investigations confirmed that all fiber contents were optimal and effective for direct usage in concrete constructions although there were some agglomeration problems for shorter fiber specimens with high fiber content.

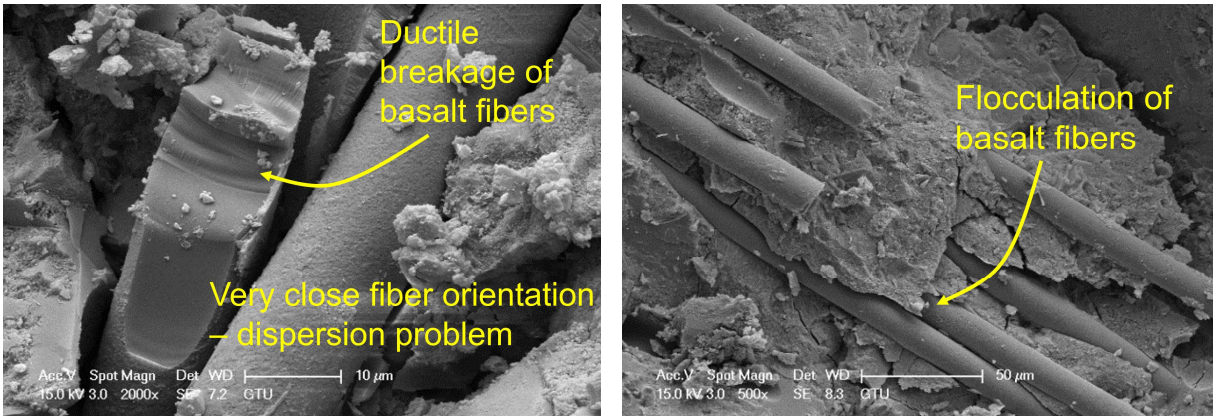

Fig. 14 - Dispersion problem detected in shorter fiber specimens.

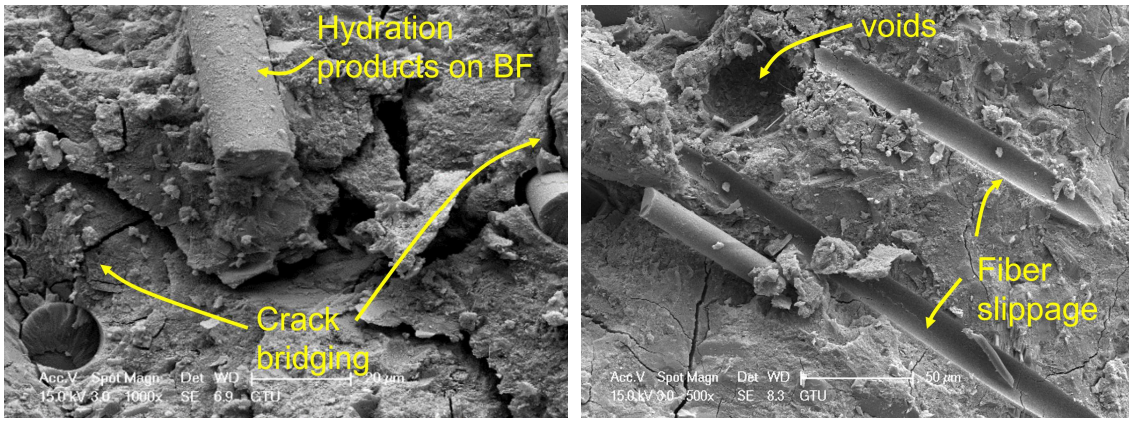

Fig. 15. (a) hydration products on basalt fibers and crack bridging (b) slipping-out of fibers

5. Conclusion

In this study, specimens with increasing content of basalt fiber in varying lengths were examined to illustrate the effect of the fibers on mechanical properties and particularly size-independent double-K parameters. For fracture toughness testing notched beam specimens were used and cracked under flexural loading and crack mouth opening displacement data was recorded simultaneously. Several findings were found for the behavior of concrete incorporating basalt fibers and given below:

Compressive strength of specimens incorporating basalt fibers were not found to be enhanced however in some specimen series, a maximum 4% increase was detected. Standard deviation results were close to plain specimens that define the proper placement despite the presence of fibers. Tensile properties showed high development for both splitting tensile and flexural testing. However, effect of the two parameters were different for flexure and splitting. Although 6 mm fiber specimens seemed more problematic for overall mechanical properties, splitting tensile results were relatively good for these short fibers. Splitting tensile and flexural test results were enhanced with 28% and 22% respectively. Modulus of elasticity results obtained from the notched three-point bending test were also in agreement with the mechanical testing results.

Highest fracture energy was measured for specimens with 1% content of 24 mm fibers displaying an increase of 37% with respect to plain specimens. Energy dissipation of shorter fibers were less compared to medium and long fibers. Double-K fracture parameters were found to be coherent with other studies in literature and these parameters demonstrated good results about fracture capability. Higher unstable toughness values proved to be a good measure of strain attaining capacity regardless of specimen size. Brittleness index also showed that fiber content was the dominant parameter regarding material toughness. Additionally, fiber length was also found to be effective in determining fracture process and energy dissipation.

REFERENCES

[1] P. Smarzewski, Flexural toughness evaluation of basalt fibre reinforced HPC beams with and without initial notch, Composite Structures, 2020, **235**, 11769.

[2] D.P. Dias, C. Thaumaturgo, Fracture toughness of geopolymeric concretes reinforced with basalt fibers, Cement and Concrete Composites, 2005, **27**, 49–54.

[3] S. Cui, X. Xu, X. Yan, Z. Chen, C.Y. Hu, Z.L. Liu, Experimental study on the interfacial bond between short cut basalt fiber bundles and cement matrix, Construction and Building Materials, 2020, **256**, 119353.

[4] S. Xu, H.W. Reinhardt, A simplified method for determining double-K fracture parameters for three-point bending tests, International Journal of Fracture, 2000, **104**, 181–209.

[5] S. Xu, H.W. Reinhardt, Determination of double-K criterion for crack propagation in quasi-brittle fracture, Part I: Experimental investigation of crack propagation, International Journal of Fracture, 1999, **98**, 111–149.

[6] A. Hillerborg, M. Modéer, P.E. Petersson, Analysis of crack formation and crack growth in concrete by means of fracture mechanics and finite elements, Cement and Concrete Research, 2008, **6** (6), 773–781.

[7] FMC-50 R, Determination of the fracture energy of mortar and concrete by means of three-point bend tests on notched beams, Materials and Structures,1985, **18**, 287–290.

[8] C. Jiang, K. Fan, F. Wu, Da Chen, Experimental study on the mechanical properties and microstructure of chopped basalt fibre reinforced concrete, Materials and Design, 2014, **58**, 187–193.

[9] N. Kabay, Abrasion resistance and fracture energy of concretes with basalt fiber, Construction and Building Materials, 2014, **50,** 95–101.

[10] T. Ayub, N. Shafiq, M.F. Nuruddin, Mechanical properties of high-performance concrete reinforced with basalt fibers, Procedia Engineering, 2014, **77**, 131–139.

[11] B. Akturk, A.H. Akca, A.B. Kizilkanat, Fracture response of fiber-reinforced sodium carbonate activated slag mortars, Construction and Building Materials, 2020, **241**, 118128.

[12] X. Sun, Z. Gao, P. Cao, C. Zhou, Y. Ling, X. Wang, Y. Zhao, M. Diao, Fracture performance and numerical simulation of basalt fiber concrete using three-point bending test on notched beam, Construction and Building Materials, 2019, **225**, 788–800.

[13] S. Kumar, S.V. Barai, Determining double-K fracture parameters of concrete for compact tension and wedge splitting tests using weight function, Engineering Fracture Mechanics, 2009, **76**, 935–948.

****